

General Disclaimer

One or more of the Following Statements may affect this Document

- This document has been reproduced from the best copy furnished by the organizational source. It is being released in the interest of making available as much information as possible.
- This document may contain data, which exceeds the sheet parameters. It was furnished in this condition by the organizational source and is the best copy available.
- This document may contain tone-on-tone or color graphs, charts and/or pictures, which have been reproduced in black and white.
- This document is paginated as submitted by the original source.
- Portions of this document are not fully legible due to the historical nature of some of the material. However, it is the best reproduction available from the original submission.

DIST. CATEGORY UC-63
DOE/JPL-955843/82/7
DRD No. SE5
DRD N. 139

LARGE-AREA SHEET TASK
ADVANCED DENDRITIC WEB GROWTH DEVELOPMENT

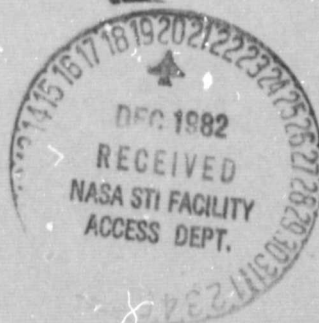
C. S. Duncan, R. G. Seidensticker, J. P. McHugh,
R. H. Hopkins, D. Meier, and J. Schruben

Quarterly Report
April 1, 1982 to June 30, 1982
Contract No. 955843

September 17, 1982

The JPL Flat Plate Solar Array Project is sponsored by the U. S. Dept. of Energy and forms part of the Solar Photovoltaic Conversion Program to initiate a major effort toward the development of low-cost solar arrays. This work was performed for the Jet Propulsion Laboratory, California Institute of Technology, by agreement between NASA and DOE.

(NASA-CR-169639) LARGE-AREA SHEET TASK N83-14669
ADVANCED DENDRITIC WEB GROWTH DEVELOPMENT
Quarterly Report, 1 Apr. - 30 Jun. 1982
(Westinghouse Research and) 40 p Unclas
HC A03/MF A01 CSCL 10A G3/44 02190



Westinghouse R&D Center
1310 Beulah Road
Pittsburgh, Pennsylvania 15235

DIST. CATEGORY UC-63
DOE/JPL-955843/82/7
DRD No. SE5
DRD N. 139

LARGE-AREA SHEET TASK
ADVANCED DENDRITIC WEB GROWTH DEVELOPMENT

C. S. Duncan, R. G. Seidensticker, J. P. McHugh,
R. H. Hopkins, D. Meier, and J. Schruben

Quarterly Report
April 1, 1982 to June 30, 1982
Contract No. 955843

September 17, 1982

The JPL Flat Plate Solar Array Project is sponsored by the U. S. Dept. of Energy and forms part of the Solar Photovoltaic Conversion Program to initiate a major effort toward the development of low-cost solar arrays. This work was performed for the Jet Propulsion Laboratory, California Institute of Technology, by agreement between NASA and DOE.



Westinghouse R&D Center
1310 Beulah Road
Pittsburgh, Pennsylvania 15235

ORIGINAL PAGE IS
OF POOR QUALITY

CONTENTS

	<u>Page</u>
LIST OF FIGURES.....	iii
1. SUMMARY.....	1
2. INTRODUCTION.....	2
3. TECHNICAL PROGRESS.....	4
3.1 Modeling.....	4
3.1.1 Model Development.....	4
3.1.2 Modeling Applications.....	9
3.2 Experimental Web Growth.....	13
3.2.1 Introduction.....	13
3.2.2 Growth Experiments.....	13
4. CONCLUSIONS.....	16
5. PLANS AND FUTURE WORK.....	17
6. NEW TECHNOLOGY.....	17
7. REFERENCES.....	18
8. ACKNOWLEDGEMENTS.....	18
9. PROGRAM COSTS.....	19
APPENDIX I. WEB TEMPERATURE COMPUTER MODEL.....	20
1. Introduction.....	20
2. Construction of Model.....	20
2.1 Differential Equation.....	20
2.2 Asymptotic Expansion.....	23
3. Computer Program Input/Output Options.....	26
APPENDIX II. COMPUTER CODE LISTING.....	29

LIST OF FIGURES

	<u>Page</u>
Figure 1 Example of numerical output from new web temperature computer code.....	6
Figure 2 Graphical output from new web temperature computer code.....	8
Figure 3 J419 configuration.....	10

PRECEDING PAGE BLANK NOT FILMED

ORIGINAL PAGE IS
OF POOR QUALITY

1. SUMMARY

The computer code for calculating web temperature distribution has been expanded to provide a graphics output for $(\alpha T)^2$ in addition to numerical and punch card output.* The new code was used to examine various modifications of the J419 configuration and, on the basis of the results, a new growth geometry was designed. Additionally, several mathematically defined temperature profiles were evaluated for the effects of the free boundary (growth front) on the thermal stress generation.

Experimental growth runs were made with modified J419 configurations to complement the modeling work. A modified J435 configuration was evaluated.

*A complete description of the computer code is included as an appendix.

ORIGINAL PAGE IS
OF POOR QUALITY

2. INTRODUCTION

Silicon dendritic web is a single-crystal silicon ribbon material which provides substantial advantages for low-cost manufacture of solar cells. A significant feature of the process is the growth from a melt of silicon without constraining dies, resulting in an oriented single-crystal ribbon having excellent surface features. In common with other more classical processes such as Czochralski growth, impurity rejection into the melt permits the use of less pure "solar grade" starting material without significantly affecting cell performance. A unique property of the dendritic web process is the growth of long ribbons of controllable width and thickness which not only facilitates automation of subsequent processing into solar cells, but also results in high material utilization since cutting and polishing are not required.

On the present contract, three broad areas of work are emphasized:

1. The development of thermal stress models in order to understand the detailed parameters which generate buckling stresses. The model can then be used to guide the design of improved low-stress web growth configurations for experimental testing.
2. Experiments to increase our understanding of the effects of various parameters on the web growth process.
3. The construction of an experimental web growth machine which contains in a single unit all the mechanical and electronic features developed previously so that experiments can be carried out under tightly controlled conditions.

Thus, the principal objective of this work has been to expand our knowledge and understanding of both the theoretical and experimental aspects of the web growth process to provide a solid base for

substantial improvements in both area throughput and web crystal quality.

During this reporting period, the new thermal model was used to examine various modifications of the J419 configuration. These results combined with experimental evaluation formed the basis for a new growth design. Work continued to optimize the J435 configuration for steady-state growth and a modified slot geometry was evaluated.

3. TECHNICAL PROGRESS

3.1 Modeling

3.1.1 Model Development

During the previous quarter, a new model was developed to calculate the temperature profile in a growing web crystal.⁽¹⁾ The objective of the new model was to provide a much higher resolution in the representation of the lid and shield geometry of the growth system which had been treated as more or less lumped blocks in the previous version. As discussed in the previous report,⁽¹⁾ the new model provides for an exact geometrical representation of each lid, shield, and spacer of a growth configuration. In this report, we discuss in more detail the input parameters available for the model as well as the output options.

Input options that are available for the model fall into two categories: selection of the operating options of the model such as type of output, number of cases, mode of integration, etc. and, second, the parameters of the configuration being analyzed. A description of the individual data cards as well as a complete listing of the program are included as an appendix to this report.

Output options available for the program fall into three categories: 1) numerical output, 2) graphics output, and 3) punched card output. The first and third output types were previously available; the second output was added when it became apparent that the second derivative of the thermal expansion coefficient times the temperature was a useful parameter for assessing the effect of changes in the shield elements on the thermal stress.

ORIGINAL PAGE IS
OF POOR QUALITY

An example of the numerical output is shown in Figure 1. The first column lists the position on the web (the growth front is at 0 cm). The second column gives the calculated temperature. The third and fourth columns are the first and second derivatives of the temperature, and the fifth column is $(\alpha T)''$. All distances are in centimeters and temperatures are in $^{\circ}\text{K}$. In addition to this data, two other sets of data are listed at the top of the printout. The first, labeled VV, is the partial growth velocity of the web resulting from the heat lost from the web crystal itself. This differs from the total growth velocity which is observed in experiments by a contribution which results from some of the latent heat being dissipated to the supercooled melt.⁽²⁾ An estimate of this total growth velocity is included as one of the input parameters to the model.

The second set of data included is an estimate of the critical yield stress for the web corresponding to the first five temperature points. The yield stress is simply an estimate based on an empirical equation from the work of Graham et al.⁽³⁾

$$\sigma_{YP} = 2.57 \times 10^{-11} \exp(49459/T) \text{ Mdyn/cm}^2 \quad (1)$$

These critical-yield stress values can be used later when actual stress distributions are generated by the finite element WECAN calculations. Although the viscoelastic phenomena responsible for the observed residual stress in the crystals is extremely complex, these data provide a first estimate of possible effects. The first four columns in the balance of the numerical data are more or less self-explanatory in being the position, the temperature, and its first two derivatives. The last column, $(\alpha T)''$, is of importance since it is basically the generating function for the thermal stress. Although the relationship between $(\alpha T)''$ and stress is not straight forward near the interface where the free boundary exerts a strong influence, it is relatively simple elsewhere where the Boley and Weiner approximation⁽⁴⁾ applies:

ORIGINAL PAGE IS
OF POOR QUALITY

$$\sigma_x = \frac{E}{6} (3y^2 - w^2) (\alpha T)'' \quad (2)$$

where E is Young's modulus and w is the half width of the ribbon. Through the relationship of T'' with the heat loss from the ribbon, it is possible to correlate the behavior of this parameter with changes in the geometry of the lids and shields.

Realization of the usefulness of the $(\alpha T)''$ parameter led to the addition of a graphics output capability to the code. Since the end application was to compare the $(\alpha T)''$ function with the geometry being analyzed, the graphics output presents both a representation of the lid and shields and the concomitant $(\alpha T)''$ curve. If the geometry does not change (lid, shield, and interface position), then up to three different $(\alpha T)''$ curves can be represented on the same plot. A representative output is shown in Figure 2; the plot of the lid and shields has been accented in the figure for the sake of emphasis.

The final output option from the program is a set of punched cards giving the nodal temperatures for use with the WECAN stress calculations. In this option, there are several sub-options depending on whether a two-dimensional stress calculation or a three-dimensional buckling calculation is to be done. Further, in the two-dimensional calculation, there is a choice as to whether quadratic or cubic elements are employed. Also, some choice is available as to some of the geometric features of the finite element grid.

Thus, the program to calculate the web temperature distribution has a great deal of flexibility in both the lid and shield configuration which can be analyzed, and in the options for presenting the results of its calculations. The flexibility of both the input and output greatly enhance the ability of the program to assist in the analysis and design of dendritic web growth configurations.

ORIGIN. N. PAGE 13
OF POOR QUALITY

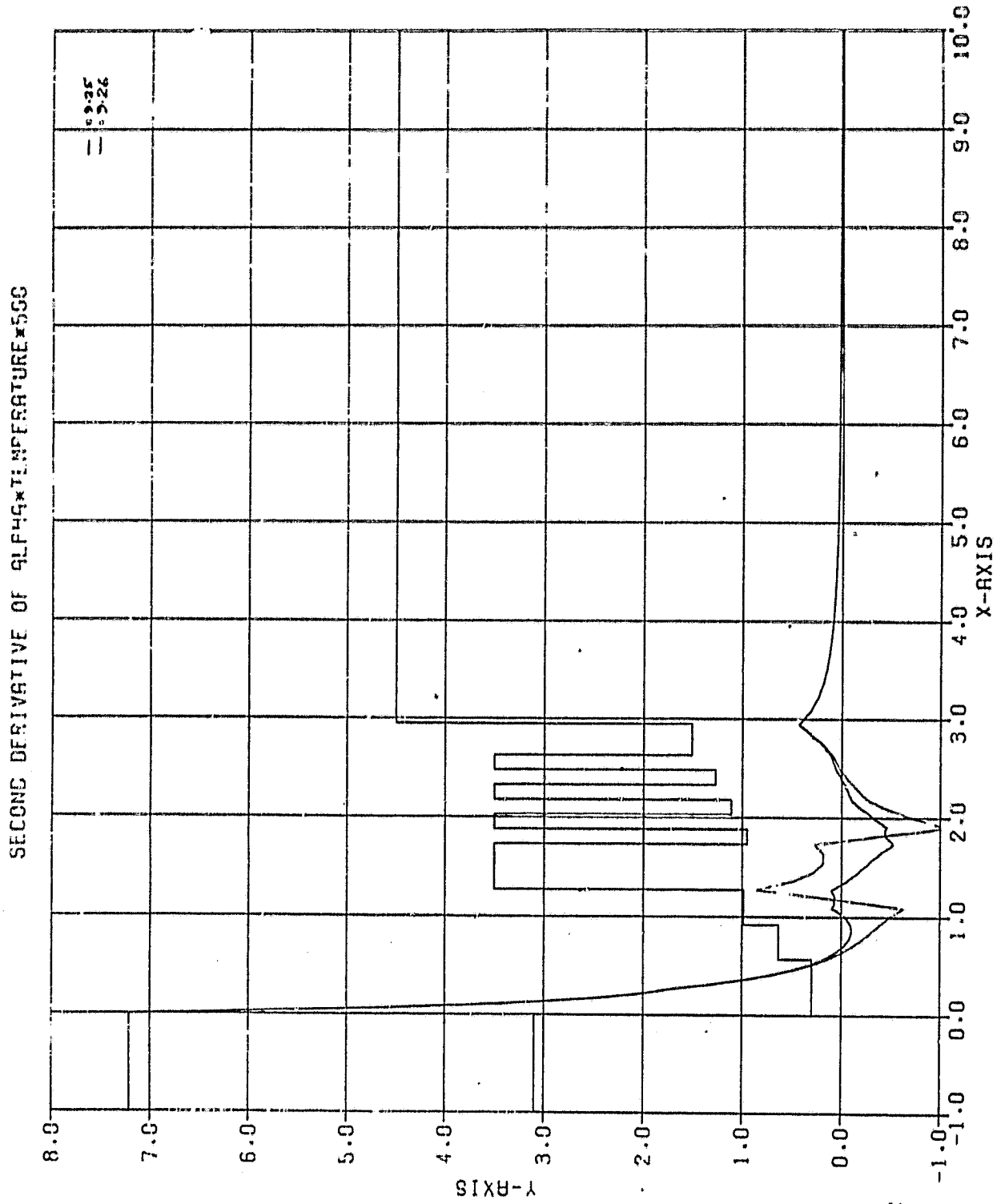


Figure 2. Graphical output from new web temperature computer code.

3.1.2 Modeling Applications

3.1.2.1 "Realistic" Growth Configurations

The first application of the new web temperature model was an evaluation of variations of the J419 configuration (Figure 3). Of course, the individual lids and shields were modeled rather than the lumped parameter "model" shown in the figure. For some of the geometries evaluated, only the (αT) curves were generated and, in these cases, the initial peak of the curve and the final, small, and maximum were the features of greatest interest. They are related respectively to the extremum in the y -stress at the growth front and to the maximum in $\Delta\sigma_x$ (difference in x -stress between center and edge) which occurs further up the crystal. In turn, these stresses are related to the residual stress in the web and to the tendency of the web to buckle.

One of the first parameters studied was the effect of work coil height as it affected the lid and shield temperatures. Temperature data were obtained from thermocouple measurements of the bottom lid and the bottom and top shields; other shield temperatures were obtained by interpolation. Although the total range of temperature change in the lid was only 18°K , the effect of changing coil position was primarily near the growth front: initial y -stress and V_w (partial web velocity). The concomitant shield temperature changes were over 60°K , but the $\Delta\sigma_x$ and the associated (αT) peak were changed very little. These results indicate that the design of the lid itself is very important in controlling both residual stress and growth speed, but does not have a great deal of control on the buckling.

As a follow-up, a beveled lid slot and a straight lid slot were compared. The beveled configuration was about 10% faster, but the initial y -stress increased about 30%. Again, minimal changes occurred in the distant $\Delta\sigma_x$ peak.

One geometrical parameter which did influence the $\Delta\sigma_x$ peak was the height of the shield stack. Increasing the separation between shields to give a higher stack not only moved the peak further away from

ORIGINAL PAGE IS
OF POOR QUALITY

Dwg. 7767A15

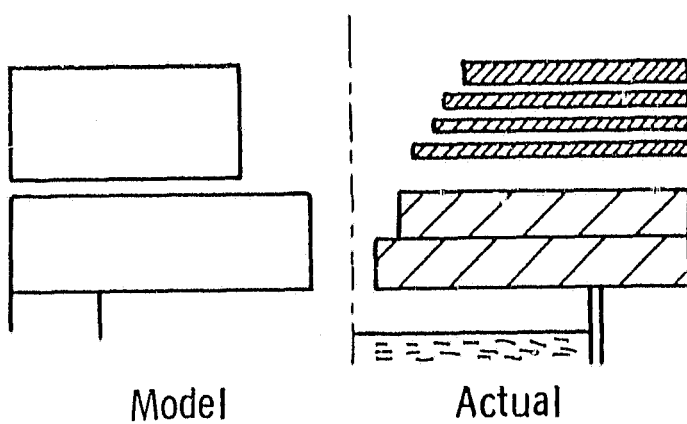


Figure 3. J419 configuration.

the interface but decreased its magnitude. All other factors being equal, this should result in a much decreased tendency to buckle.

Other geometrical parameters investigated were the width of the lid slot, the view angle through the shield stack, and the effect of solid spacers between the shields, etc. It was found that decreasing the slot width should increase the growth speed as does opening the view angle. All of these factors also tend to increase the initial y-stress, so that there is a trade-off in arriving at any final design.

On the basis of all the factors studied, a new proposed growth configuration was designed and constructed. This design, called the "J460" configuration (after its first trial run), was anticipated to have low buckling tendency, although the residual stress was uncertain. In fact, as discussed elsewhere, this proved to be a very successful configuration.

3.1.2.2 Synthetic Temperature Profile

In addition to modeling existing or hypothetical lid and shield configurations, stresses were calculated for two "synthetic" temperature profiles that were defined as purely mathematical functions. The goal of these test cases was to obtain an estimate, and perhaps at least a semiquantitative representation of the free-boundary end effect. The region near the growth front is of prime importance in the generation of plastic deformation in the web crystals and yet is a region of least theoretical guidance in relating the temperature profile to the thermal stresses.

The first synthetic temperature profile was a rerun of the constant stress profile discussed in a previous report.⁽⁵⁾ Although the previous results were close to those predicted from simple analytical considerations, there were several aspects where they differed. At first, this was attributed to numerical effects in the WECAN program, but then it was realized that the finite element grid had edge elements which modeled the bounding dendrites and would cause the stress fields

ORIGINAL PAGE IS
OF POOR QUALITY

to depart from the ideal case of a flat ribbon. The temperature profile was re-analyzed using a mesh for a simple ribbon, and the results were now in perfect agreement with the theoretical predictions.

As before, the effect of the free boundary extended into the crystal for a distance approximately equal to the full ribbon width. As an approximation, the x-stress varied as $1 - \exp(-x^2/w^2)$, where w = ribbon half width. Using this relation as an admittedly approximate guideline, it is possible to assess the relative effects of features in the (αT) profile near the interface.

The second synthetic temperature profile assumed an exponential decay of the (αT) profile from its value near the interface. This particular function was chosen since it is a reasonable approximation to the behavior observed in models of any realistic lid/shield configurations, although in those cases, the exponential behavior is found only in the first 5 mm or so. The stress distribution from the synthetic temperature case was in reasonable quantitative agreement with the stress distributions in the interface region of the more realistic cases, although of course the more distant features were quite different. In both the synthetic and realistic cases, the actual x-stress magnitude near the boundary was far smaller than might be anticipated, in agreement with the boundary effect of the constant stress case. These results indicate that the initial (αT) peak is responsible for much of the thermal stress behavior at the interface, but also that there are other factors such as the free boundary effect which must be considered. It is also not yet clear to what effect the peak height and the characteristic decay length of the exponential are involved in the stress generation. These factors need some additional runs to clarify the behavior. The final results should be applicable to the design of lid configurations for faster growth with lower residual stress.

3.2 Experimental Web Growth

3.2.1 Introduction

The process of developing a functional new growth configuration follows a three-stage progression. The first stage is the thermal modeling, the results of which generate a design for a growth configuration. Stress and buckling models are applied as appropriate when the (αT)" results warrant the effort. The design is then fabricated into hardware and tested experimentally. The objective of this second phase of the progression is to experimentally verify the stress behavior predicted by the model, i.e., to find how wide the crystal can grow before deformation occurs. At this stage, long slots which provide melt temperature profiles compatible with crystal widths of about 6.5 cm are used. Lid and shield temperature measurements are made to verify consistency with the model, and modifications are made as required to produce the desired temperature distribution in the vertical direction. This stage involves a cross interaction between modeling and experiment. The third stage of development is the adaptation of the low-stress configuration for semi-automated growth. This phase is largely empirical, guided by experience. It involves the incorporation of melt replenishment and width control provisions into the design, and the determination of optimum shielding and coil position for good growth at constant width and melt level, i.e., steady-state growth. Only the designs which continue to show promise through the first and second phases reach the third phase.

3.2.2 Growth Experiments

A series of variations of the J419 configuration were tested in order to evaluate the effects on growth of changes in top shield spacing and minor variations in slot geometry and coil position, etc. Lid and shield temperature measurements were made to complement the modeling work. Growth parameters evaluated were growth velocity and residual stress, in addition to the width at which buckling was initiated.

In general, the only modification of the basic design which had a positive effect on growth was a small bevel on the lid slot. Other variations either had little observable effect on growth behavior or generated a negative result. For example, opening the slots in the top shields increased the growth velocity but caused the crystal to degenerate at narrower widths. The model indicated that increasing the height of the top shield stack should further reduce buckling stresses, but this did not seem to have a significant effect with the J419 lid configuration. Finally, on the basis of modeling results and the experimental correlations, it was concluded that a new lid slot geometry combined with an extended shield stack should produce significantly lower buckling stresses than the J419 configuration. The required hardware has been fabricated and the design will be fully evaluated during the next reporting period. However, preliminary indications are that the new design is indeed a major step forward in stress reduction and width enhancement.

In parallel with the above effort, experimental growth runs with the J435 configuration (which combines the low-stress aspects of the J419 with the width-limiting capabilities of the J98M3) were continued in the N-furnace. The objective was to optimize the furnace parameters for steady-state growth. The parameters to be determined include coil height, end shield positions, and melt level.

Having adjusted these parameters, a number of crystals was grown 3 to 4 meters long with the width consistently saturating at 3.3 cm, the design target for this configuration. However, at this width, a considerable portion of either edge of the web is growing in the dog bone region of the slot, i.e., the full face of the web does not see a uniform slot width. This results in a visible change in the web surface along the edges as compared with the central region. In an effort to improve surface uniformity, a modified lower lid was fabricated without dog bones in the growth region, i.e., a straight slot.

ORIGINAL PAGE IS
OF POOR QUALITY

The surface of web grown with this straight slot was extremely flat and uniform. However, the web crystals widened slowly and were subject to pullout if not closely monitored by the furnace operator. In one run, a 4.3 meter long, 3.4 cm wide crystal was grown, but this was the exception rather than the rule. Thus, although the straight slot produces a beautiful crystal surface, it is difficult to grow a crystal at full width. We plan a further modification such that at full width, only the dendrites see the open lid environment, while the full face of the web sees a uniform slot. This arrangement should improve growth stability while maintaining uniform surface quality.

ORIGINAL PAGE IS
OF POOR QUALITY

4. CONCLUSIONS

The new thermal model has proved a valuable tool in its ability to accommodate complex lid and shield configurations. Its application to modifications of the J419 configuration along with experimental input has led to a new design for a low-stress growth configuration in a systematic manner.

Semi-automated web growth has been demonstrated with the J435 configuration in the N-furnace, although we are not yet satisfied that this basic configuration is fully optimized for long-term steady-state growth. Further trimming of this configuration will continue in parallel with evaluation of the new design aimed at much greater crystal width.

ORIGINAL PAGE IS
OF POOR QUALITY

5. PLANS AND FUTURE WORK

The computer code will be used for further evaluation of a new lid design and the buckling behavior of the configuration will be calculated. The new lid design will be evaluated experimentally and modified as required.

6. NEW TECHNOLOGY

No new technology is reportable for the period covered.

ORIGINAL PAGE IS
OF POOR QUALITY

7. REFERENCES

1. C. S. Duncan et al., Large-Area Sheet Task: Advanced Dendritic Web Growth Development, Quarterly Report (August 18, 1982), DOE/JPL-955843/82/6.
2. C. S. Duncan et al., Silicon Web Process Development: Annual Report (June 30, 1980), DOE/JPL-954654/80/11, p. 44.
3. C. S. Duncan et al., Silicon Web Process Development: Annual Report (January 4, 1979), DOE/JPL-954654/79/2, p. 122.
4. B. A. Boley and J. H. Weiner, Theory of Thermal Stresses (New York: Wiley, 1960), p. 323.
5. C. S. Duncan et al., Large-Area Sheet Task: Advanced Dendritic Web Growth Development, Quarterly Report (June 18, 1982), DOE/JPL-955843/82/5, p. 5.

8. ACKNOWLEDGEMENTS

We would like to thank H. C. Foust, E. P. A. Metz, L. G. Stampahar, S. Edlis, W. B. Stickel, and W. Chalmers for their contributions to the web growth studies.

ORIGINAL PAGE NO
OF POOR QUALITY

9. PROGRAM COSTS

9.1 Man-Hours and Costs

Man-Hours		Costs	
Previous	27,682	Previous	\$1,232,077
This Quarter	3,415	This Quarter	162,088
Cumulative	31,097	Cumulative	\$1,394,165

ORIGINAL PAGE 13
OF POOR QUALITY

APPENDIX I

Web Temperature Computer Model

1. INTRODUCTION

Thermal stress and buckling modeling of dendritic web crystals requires temperature distribution data along the growing web. Because of the difficulty of measuring web temperature, we instead compute it from the furnace lid and shield geometry and temperature distribution. This computation is performed by a computer code called "RIBBON" which integrates the required heat transfer equation for the given radiative web environment. A description of this program and data input follows.

2. CONSTRUCTION OF MODEL

2.1 Differential Equation

The purpose of the RIBBON program is to determine the temperature, T , of the growing silicon web as a function of the distance, x , from the lower edge of the furnace lid. RIBBON accomplishes this task by integrating the heat conduction equation:

$$\rho C_p V \frac{dT}{dx} = \frac{d}{dx} \left(\frac{a}{T} \frac{dT}{dx} \right) - \frac{2q}{b} \quad [A-1]$$

where ρ = density

C_p = specific heat

V = web pull velocity

a = 318 W/cm

b = web thickness

q = heat flux from one side of the web.

One of the major tasks of the RIBBON program is to calculate the geometric form factors for the term "q". A detailed discussion of this computation is found in the last quarterly report (DOE/JPL-955843/82/6). For the purpose of recognizing the degree of nonlinearity of equation A-1, we note that q can be expressed in the form

$$q = \sigma E T^4 + f(x),$$

where σ is the Stephan-Boltzman, E is the emissivity of silicon web, and $f(x)$ is a function of position x on the web and the geometry and temperatures of the lid and shields of the furnace. Above 20 cm from the lid, the web enters a chimney and thus no longer "sees" the lid and shields. For a simple approximation, we say that it "sees" only the ambient temperature, T_a . Thus, for $x \geq 20$ cm,

$$q = \sigma \epsilon (T^4 - T_a^4) \quad [A-2]$$

The longer the ribbon grows, the closer its temperature approaches the ambient. This fact together with the initial condition that the web starts to grow at the silicon melt temperature, $T_m = 1685^\circ\text{K}$, gives us the boundary conditions

$$\begin{aligned} T(x_0) &= T_m \\ T(\infty) &= T_a \end{aligned} \quad [A-3]$$

The position $x = x_0$ is the growth front and has a value equal to the negative of the input parameter LIN in the program.

Differential equations with boundary conditions are more difficult to solve than those with initial conditions; they generally must be solved iteratively. Since most numerical integration routines are written for first order equations, we transform the second order equation (A-1) into two first order equations with the substitutions:

ORIGINAL PAGE IS
OF POOR QUALITY

$$\begin{aligned}
 u_2 &= \rho C_p V T_m/a \\
 \beta_2 &= \epsilon \sigma T_m^4/(ab) \\
 TT(1) &= T/T_m \\
 TT(2) &= \frac{dT}{dx} (1/T) \qquad [A-4]
 \end{aligned}$$

Equation A-1 can be expressed now as a system of first order equations:

$$\begin{aligned}
 TTP(1) &= TT(1) \cdot TT(2) \\
 TTP(2) &= u_2 TTP(1) + \beta_2 Q
 \end{aligned}$$

where

$$TTP(i) = \frac{d}{dx} [TT(i)] \quad i = 1, 2$$

and

$$Q = 2q/\epsilon\sigma \quad [A-5]$$

The nonlinearity of these equations makes them unstable as small errors in the steps of the integration are quickly magnified in the succeeding steps. We tried several different methods of numerical integration but found the simple fourth order Runge-Kutta method to be the most stable. Even so it is necessary to use double precision to obtain reasonable results. In practice, an initial slope of the temperature is guessed. If the slope leads to a curve which gives below the ambient temperature, then the slope is increased for the next guess. If the resulting curve goes above the silicon melt temperature, then the initial slope is decreased. This iteration continues until the double precision accuracy of the choice of initial slope is exhausted; in other words, there is no way to choose an initial slope between the high slope and the low slope since they are identical to 16 places. Generally, the integration curve does not blow up (or down) until 20 - 30 cm. In this case the integration from 0 to 10 cm (the length of the buckling finite element model) is fairly accurate. If it blows up before this length, this may no longer be true. (A smaller integration

step size, HO , may improve this problem.) Also, if the integration remains between the melt and ambient temperature for a longer length, the integration may not be accurate because other values of the initial slope may lead to different temperature curves which also remain bounded. The boundary condition, $T(\infty) = T_a$, must then be applied. Thus, it becomes necessary to examine the asymptotic expansion of equations A-1 and A-2. While the numerical integration of equation A-1 or equation A-4 starting with initial values at the melt interface will be accurate for small values of x , the asymptotic expansion can be expected to be accurate for large values of x . Hopefully, their regions of accuracy will overlap; if this is not the case for some problems, then some approximation to an intermediate solution might be required.

2.2 Asymptotic Expansion

For large x , it is most convenient to change the differential equations A-1 and A-2 into a system of first order equations with the following substitutions:

$$\begin{aligned}\alpha &= \rho C_l T_a / a \\ \gamma &= 2\epsilon\sigma T_a^4 / abc^2 \\ y_1 &= T/T_a \\ y_2 &= (1/\alpha T) \frac{dT}{dx}\end{aligned}\tag{A-6}$$

Thus,

$$\begin{aligned}\frac{dy_1}{dx} &= \alpha y_1 y_2 \\ \frac{dy_2}{dx} &= \alpha y_1 y_2 + \gamma\alpha (y_1^4 - 1)\end{aligned}\tag{A-7}$$

If one attempts a formal power series solution of equation A-7 in negative powers of x (so that they are finite as x approaches infinity), one would obtain the trivial solution $Y_1 = 1$ and $Y_2 = 0$. This solution,

however, does not give the general asymptotic expansion of equation A-7. Theory (Wolfgang Wason, Asymptotic Expansions for Ordinary Differential Equations, Interscience, N.Y., 1965) shows that the general solution is a function of two parameters: $C \exp \alpha x(1-\sqrt{1+16\gamma})/2$ and $D \exp \alpha x(1+\sqrt{1+16\gamma})/2$, where C and D are arbitrary constants. Since the second parameter becomes infinite as x approaches infinity, we let D vanish and look for functions of the first parameter. The substitution

$$\xi = \exp [\alpha x(1-\sqrt{1+16\gamma})/2]$$

transforms the equation A-6 into

$$\begin{aligned} y_1' \xi (1 - \sqrt{1+16\gamma}) &= 2 y_1 y_2 \\ y_2' \xi (1 + \sqrt{1+16\gamma}) &= 2 y_1 y_2 + 2\gamma (y_1^4 - 1) \end{aligned} \quad [A-8]$$

where the primes represent differentiation with respect to the variable ξ . We can now seek a power series solution of equation A-8 in the form

$$\begin{aligned} y_1 &= a_{10} + a_{11} (C\xi) + a_{12} (C\xi)^2 + \dots \\ y_2 &= a_{21} (C\xi) + a_{22} (C\xi)^2 + \dots \end{aligned} \quad [A-9]$$

where $a_{10} = 1$ from the boundary condition and a_{11} may also be chosen equal to unity since C is an arbitrary constant. Equating the coefficients of $(C\xi)^n$ on both sides of equation A-8, we obtain

$$\begin{aligned} n a_{1n} (1 - \sqrt{1+16\gamma}) &= 2 \sum_{m=0}^{n-1} a_{1m} a_{2(n-m)} \\ n a_{2n} (1 + \sqrt{1+16\gamma}) &= 2 \sum_{m=0}^{n-1} a_{1m} a_{2(n-m)} + 2\gamma [b_{n/2}^2 + 2 \sum_{m=0}^{(n/2)-1} b_m b_{n-m}] \end{aligned} \quad [A-10]$$

ORIGINAL PAGE IS
OF POOR QUALITY

for n even or

$$na_{2n} (1 - \sqrt{1+16\gamma}) = 2 \sum_{m=0}^{n-1} a_{1m} a_{2(n-m)} + 4\gamma \sum_{m=0}^{(n-1)/2} b_m b_{n-m} \quad [A-10]$$

for n odd,

where

$$b_i = a_{1(i/2)}^2 + 2 \sum_{j=0}^{i/2-1} a_{1j} a_{1(i-j)}, \quad i \text{ even}$$

$$= \sum_{j=0}^{(i-1)/2} a_{1j} a_{1(i-j)}, \quad i \text{ odd}$$

$$b_0 = 1$$

From these equations, the a_{1n} and a_{2n} are determined from the values of a_{1m} and a_{2m} , where $m < n$. In this way, we find the coefficients of the asymptotic expansion A-9. The radii of convergence of these power series may be found from the formulas:

$$R = \lim | a_n / a_{n+1} | \text{ if it exists}$$

$$\text{and } \lim_{n \rightarrow \infty} \sup | a_n |^{1/n} = \alpha = 1/R$$

The next steps in the procedure are to choose a value of C and then a value of $\xi > 20$ cm. such that equation A-9 converges. From equations A-4, A-6, and A-9, initial conditions for equation A-5 may be found at the value of x corresponding to that of ξ . Equation A-5 can now be integrated backward to $x = x_0$ using the same Runge-Kutta method as before. These steps are iterated by increasing or decreasing the choice of C accordingly as $T(x_0)$ is less than or greater than T_m .

3. COMPUTER PROGRAM INPUT/OUTPUT OPTIONS

The input parameters of the RIBBON program are divided into two sets -- the first to define the geometry and the second everything else. In this way, Calcomp plots may be obtained for any number of geometric configurations in each run. In each plot, up to three different graphs (black, green, and red) of the second derivative of αT can be obtained for different nongeometric parameters of web growth run.* A sample Calcomp plot is illustrated in Figure 2. Besides the αT second derivative curves, it diagrams the lid and shield geometry.

The following input records are read in the first data set. The data are read in free field format with either spaces or commas separating them. Variables beginning with I-N are integer. (except for LIN) and all others are double precision.

RECORD 1:

IGRAPH = Input 0 if there are to be no Calcomp graphs in the run, otherwise input 1.

RECORD 2:

NS = Number of geometric elements. These include the lid, the shields, and their separating gaps.

JQC = Parameter to correspond to the type of WECAN element

= 2 for quadratic elements

= 3 for cubic elements

JN = Number of WECAN elements in the x direction (generally has been set to 23).

NE = Number of WECAN elements in the y direction (generally has been 5 for two-dimensional elements and 7 for three-dimensional ones).

*Here α stands for the thermal expansion of silicon and is represented by $ALPO + ALPI * TEMP$ in the program; it is unrelated to the α in equations A6 and A7.

ORIGINAL PAGE IS
OF POOR QUALITY

NG = One plus the number of data sets for a given geometry.

LIN = Distance (cm) of the growth front below the lower edge of the lid.

EMAG = Magnification of the JNth element in the x direction relative to the first WECAN element at the growth front (generally has been 8).

ELL = Length of ribbon modeled on WECAN in centimeters (generally has been 10).

RECORD 3:

H(I), I = 1, .NS = Height (cm) of ith horizontal surface above the lower surface of the lid.

RECORD 4:

Y(I), I = 0, ..., NS+1 = Half width (cm) of the central gap of the ith horizontal surface.

The H and Y parameters are illustrated in Figure 3. This completes the first data set.

The second data set consists of the following records:

RECORD 1:

IS = 1 for forward integration
= -1 for backward integration from asymptotic expansion (not yet implemented).

HO = integration step size (generally set to 0.01).

KOUT = 6 for printed temperature data in WECAN stress input formalism
= 7 for punched WECAN data.

KOU = 0 for no plot of the αT second derivative.
= 1 for a plot

EPS = emissivity of silicon web.

ORIGINAL PAGE IS
OF POOR QUALITY

- A = thermal conductivity of silicon multiplied by its temperature
(318 W/cm).
- B = web thickness (cm).
- V = web pull velocity (cm/min)
- POMIN = minimum initial value of TT(2). If not known, set to -1.
- POMAX = maximum initial value of TT(2). If not known, set to -0.01.
- CMIN = minimum value of the parameter in equation (A-9). If not known,
try 1.
- CMAX = maximum value of the parameter C. If not known, try 20.

RECORD 2:

TS(I), I = 1, ... , NS+1 = Temperature (degrees Kelvin) of the ith
geometric element.

These RECORDS 1 and 2 may be repeated up to a total of three sets. The
data sets 1 and 2 can be repeated an indefinite number of times.

ORIGINAL PAGE IS
OF POOR QUALITY

APPENDIX II
Computer Code Listing

@RUN, /RNPT JSS05,09F40READY20,SCHRUBEN,5,100/1500

@HDG RIBBON

@FTN,SDFIV
FTN 8RTW4

08/25/82-20:50

```

1. C SILICON WEB - ANALYSIS OF HEAT LOSS OF MOVING WEB
2. IMPLICIT DOUBLE PRECISION (A-H,O-Z)
3. DOUBLE PRECISION LIN,LAMB,TS(0:20),H(0:20),Y(0:20),XS(0:100),
4. X(0:60)
5. 1 DIMENSION TT(2),TS4(20),T(100),TP(100),TPP(100),ATPP(100),Y2((
6. ,TPP(2)
7. 1 INTEGER IXS(40),ISR(0:60,20)
8. INTEGER TITLE(11),LABELX(2),LABELY(2),ICOLOR(4)
9. REAL XR(150),YR(4,150),XLEN
10. C THE ABOVE ARE GRAPH PARAMETERS
11. COMMON /CNI/ U2,BETA2,ISR,TS4,Y2,H,ICHIM,NS,NS1
12. COMMON /CNJ/ TA,IFLAG
13. DATA TITLE/'SECO','ND D','ERIV','ATIV','E OF','ALP','HA*T',
14. 'EMPE','RATU','RE*5','00'/
15. 1 DATA LABELX/'X-AX','IS'
16. DATA LABELY/'Y-AX','IS'
17. DATA ICOLOR/1,1,2,3/
18. KI= 5
19. KO= 6
20. C IGRAPH = 0 FOR NO CALCOMP
21. = 1 FOR SOME CALCOMP
22. C NG IS ONE PLUS NUMBER OF DATA SETS FOR A GIVEN GEOMETRY (4 MA)
23. NS IS NUMBER OF SHIELDS PLUS LID SECTIONS PLUS GAPS INBETWEEN
24. C TS(I) IS THE TEMPERATURE OF THE ITH SHIELD OR GAP
25. H(I) IS THE HEIGHT OF THE ITH HORIZONTAL SURFACE ABOVE THE LOI
26. C SURFACE OF THE LID
27. Y(I) IS THE DISTANCE OF SHIELD EDGE TO WEB
28. C (Y(0) IS HALF-WIDTH OF MELT SURFACE, Y(1) IS HALF GAP OF LID,,
29. Y(NS) IS DISTANCE OF INNER EDGE OF TOP SHIELD TO WEB,
30. C Y(NS+1) IS DISTANCE OF OUTER EDGE OF TOP SHIELD TO WEB)
31. JQC=2 FOR QUADRATIC ELEMENTS
32. =3 FOR CUBIC ELEMENTS
33. C IS=1 FOR FORWARD INTEGRATION
34. =-1 FOR BACKWARD INTEGRATION
35. JN IS NUMBER OF ELEMENTS IN A ROW ALONG THE WEB AXIS
36. C LIN IS DISTANCE OF GROWTH FRONT BELOW LID
37. -LIN .GT. X(0)
38. C EMAG IS MAGNIFICATION OF LAST ELEMENT RELATIVE TO FIRST NEXT 1
39. ELL IS LENGTH OF WEB TO BE MODELED
40. C WE ASSUME ELL < 20
41. NE= 5 FOR 2D ELEMENTS
42. NE= 7 FOR 3D ELEMENTS
43. TS(0)= 1685.00
44. TM= 1685.00
45. TMR= 1./TM
46. LAMB= 1804.00
47. TM4= TM**4
48. CP= 0.981100
49. RHO= 2.3000
50. SIGMA= 5.67D-12
51. H(0)= 0
52. X(0)= -1
53. ISR(0,0)= 0
54. XO= X(0)
55. ISR(0,1)= 1
56. XS(0)= XO
57. READ(KI,*) IGRAPH
58. IF (IGRAPH .GT. 0) CALL PLOTIN(1.,1.)
59. YR(1,1)= -1
60. XR(1)= -1
61. XR(2)= -1
62. DO 998 ISUPER=1,10
63. READ(KI,*,END=999) NS,JQC,JN,NE,NG,LIN,EMAG,ELL
64. WRITE(KO,5) NS,JQC,JN,NE,NG,LIN,EMAG,ELL
65. 5 FORMAT('0 NS=',I4,' JQC=',I4,' JN=',I4,' NE=',I4,' NG=',I4,
66. ' LIN=',E12.5,' EMAG=',E12.5,' FLL=',E12.5)
67. 1 NS1= NS+1
68. H(NS1)= 20

```

ORIGINAL PAGE IS
OF POOR QUALITY

RIBBON

```

1 60 READ(KI,*) (H(I),I=1,NS)
2 70 WRITE(KO,7) (H(I),I=1,NS)
3 71 FORMAT('OH= ',(E14.5))
4 72 READ(KI,*) (Y(I),I=0,NS1)
5 73 WRITE(KO,8) (Y(I),I=0,NS1)
6 74 FORMAT('OY= ',(D14.5))
7 75 DO 10 I=0,NS1
8 76 Y2(I)=Y(I)**2
9 77 CONTINUE
10 78 YR(1,2)=SNGL(Y(0))
11 79 ALP0=2.8457E-6
12 80 ALP1=9.796E-10
13 81 ALP2=2*ALP1
14 82 K=0
15 83 DO 50 I=2,NS
16 84 I1=I-1
17 85 XLS=XO
18 86 XLS IS THE LOWER BOUND OF TS(I) RADIATION ON WEB
19 87 HI=H(I)
20 88 YI=Y(I)
21 89 DO 20 J=1,I1
22 90 IF (YI .GT. Y(J)) THEN
23 91 TEMP=(H(J)*YI-Y(J)*HI)/(YI-Y(J))
24 92 IF (TEMP .GT. XLS) XLS=TEMP
25 93 END IF
26 94 CONTINUE
27 95 IF (XLS .LE. XO) THEN
28 96 ISR(0,I)=1
29 97 ELSE
30 98 ISR(0,I)=-1
31 99 DO 25 J=K,0,-1
32 100 J1=J+1
33 101 IF (XLS .GE. XS(J)) THEN
34 102 XS(J1)=XLS
35 103 IXS(J1)=I
36 104 GO TO 26
37 105 ELSE
38 106 XS(J1)=XS(J)
39 107 IXS(J1)=IXS(J)
40 108 END IF
41 109 CONTINUE
42 110 K=K+1
43 111 END IF
44 112 XUS=20
45 113 XUS IS THE UPPER BOUND OF TS(I1) RADIATION ON WEB
46 114 HI=H(I-2)
47 115 YI=Y(I1)
48 116 DO 30 J=1,NS
49 117 J1=J-1
50 118 IF (YI .GT. Y(J)) THEN
51 119 TEMP=(YI*H(J1)-HI*Y(J))/(YI-Y(J))
52 120 IF (TEMP .LT. XUS) XUS=TEMP
53 121 END IF
54 122 CONTINUE
55 123 IF (XUS .LT. 20) THEN
56 124 DO 35 J=K,0,-1
57 125 J1=J+1
58 126 IF (XUS .GE. XS(J)) THEN
59 127 XS(J1)=XUS
60 128 IXS(J1)=I1
61 129 GO TO 36
62 130 ELSE
63 131 XS(J1)=XS(J)
64 132 IXS(J1)=IXS(J)
65 133 END IF
66 134 CONTINUE
67 135 K=K+1
68 136 END IF
69 137 CONTINUE
70 138 IB=0
71 139 I=0
72 140 DO 70 L=1,K
73 141 IF (XS(L)-X(I) .LT. 1.0-4) THEN
74 142 IXSL=IXS(L)
75 143 ISR(I,IXSL)=-ISR(I,IXSL)
76 144 GO TO 70

```


ORIGINAL PAGE IS
OF POOR QUALITY

RIBBON

2998
2999
3000
3001
3002
3003
3004
3005
3006
3007
3008
3009
3010
3011
3012
3013
3014
3015
3016
3017
3018
3019
3020
3021
3022
3023
3024
3025
3026
3027
3028
3029
3030
3031
3032
3033
3034
3035
3036
3037
3038
3039
3040
3041
3042
3043
3044
3045
3046
3047
3048
3049
3050
3051
3052
3053
3054
3055
3056
3057
3058
3059
3060
3061
3062
3063
3064
3065
3066
3067
3068
3069
3070
3071
3072

```

TPP(I) = TEMPPP
ATPP(I) = ATEM
450 IF (MOD(I,JQC) .EQ. 151) DX = DX*RA**IS
CALL FCNI(X2,TT,TTP,K)
I3 = I2+IS
T(I3) = TT(1)*TM
I = I3
XS(I) = X2
TP(I) = TT(2)*T(I)
TPP(I) = T(I)*(TT(2)**2+TTP(2))
ATPP(I) = (ALP0+ALP2*T(I))*TPP(I)+ALP2*TP(I)**2
XR(KK) = SNGL(X2)
YR(IC,KK) = AMAX1(-1.,AMIN1(8.,SNGL(ATPP(I))+500.))
IF (IS .EQ. -1) GO TO 600
DO 500 JK = K,LAS
IF (JK .EQ. LAS) ICHIM = 0
CALL FCNJ(X2,X(JK),TT,TTP,HO,JK)
IF (IFLAG .NE. 0) GO TO 600
X2 = X(JK)
500 CONTINUE
600 CONTINUE
780 WRITE(KO,1002) IFLAG
1005 WRITE(KO,1005) X1,X2,TT,P00,C
FORMAT(3D25.18)
IF (IS .EQ. -1) GO TO 95
IF (IFLAG) 93,92,94
92 GO TO 102
93 P0MIN = P00
GO TO 101
94 P0MAX = P00
GO TO 101
95 CONTINUE
101 CONTINUE
102 VV = -60*A* P00/(RHO*LAMB)
7100 WRITE(KO,7100) VV
FORMAT(1,5X,'VV = ',E14.7)
DO 849 I = 1,5
YIELD = 2.57E-11*EXP(49459/T(I))
849 WRITE(KO,8490) YIELD
8490 FORMAT('YIELD = ',E15.8)
DO 852 I = 1,JNN
852 WRITE(KO,1000) XS(I),T(I),TP(I),TPP(I),ATPP(I)
DO 850 I = 1,JN
II = JQC*(I-1)+1
T1 = T(II)
T2 = T(II+1)
T3 = T(II+2)
T4 = T(II+3)
DO 800 J = 1,NE
II = J+(I-1)*NE
IF (JQC .EQ. 3) GO TO 795
WRITE(KOUT,1006) II,T1,T1,T3,T3,T1
IF (NE .EQ. 5) THEN
WRITE(KOUT,1008) T2,T3,T2
ELSE
WRITE(KOUT,1007) T1,T3,T3,T1,T2,T3,T2,T1,T1,T3
WRITE(KOUT,1008) T3,T1,T2,T3,T2
END IF
GO TO 800
795 WRITE(KOUT,1006) II,T1,T1,T4,T4,T1
WRITE(KOUT,1007) T2,T4,T3,T1,T3
WRITE(KOUT,1008) T4,T2
800 CONTINUE
850 CONTINUE
YR(IC,1) = 8
DO 860 KKI = 2,KKS
YR(IC,KKI) = YR(IC,KKS+1)
860 CONTINUE
997 CONTINUE
ISW = -1
K = KKKS-1
DO 865 KKI = KKS1,KK
IF (XR(KKI) .NE. SNGL(H(K))) THEN
YR(1,KKI) = YR(1,KKI-1)
ELSE
K = K + MAXU(0,ISW)

```

ORIGINAL PAGE IS
OF POOR QUALITY

DATE 0

RIBBON

3
3
3
2
2
1
1
1
1
1

```
373. YR(1,KKI)= SINGL(Y(K))
374. ISW= -ISM
375.
376. END IF
377. CONTINUE
378. DO 866 I= 1,KK XR(I), (YR(J,I),J=1,NG)
379. WRITE(KO,1000) I, KK XR(I), (YR(J,I),J=1,NG)
380. XLEN= 1.-SINGL(LIN)+ELL
381. IF (KOU .GT. 0) CALL GRAPH(XR,YR,NG,4, KK,XLEN,9,0,0,TITLE,42,
1 LABELX,6,LABELY,6,0,0,ICOLOR)
382.
383. CONTINUE
384. IF (IGRAPH .GT. 0) CALL PLOT(0,0,0,999)
385. FORMAT(8D15.8)
386. FORMAT(7(D15.8,I3))
387. FORMAT(30I4)
388. FORMAT(I6,12X,5F12.4,+)
389. FORMAT(18X,5F12.4,+)
390. FORMAT(18X,5F12.4)
391. FORMAT(8E15.8)
392. CALL EXIT
393. ENDS
```

ORIGINAL PAGE IS
OF POOR QUALITY

RIBBON

FORM-1111-1

```
373.          YR(1,KKI)= SNGL(Y(K))
374.          ISW= -ISW
375.      END IF
376.      865 CONTINUE
377.      DO 866 I= 1,KK
378.      866 WRITE(KO,1009) XR(I), (YR(J,I),J=1,NG)
379.          XLEN= 1.-SNGL(LIN) +ELL
380.          IF (KOU .GT. 0) CALL GRAPH(XR,YR,NG,4,KK,XLEN,9.,0,0,TITLE,
381.          LABELX,6,LABELY,6,0,0,ICOLOR)
382.      998 CONTINUE
383.      999 CONTINUE
384.      IF (IGRAPH .GT. 0) CALL PLOT(0.,0.,999)
385.      1000 FORMAT(8D15.8)
386.      1001 FORMAT(7(D15.8,I3))
387.      1002 FORMAT(30I4)
388.      1006 FORMAT(I6,12X,5F12.4,4(+-)
389.      1007 FORMAT(18X,5F12.4,4(+-)
390.      1008 FORMAT(18X,5F12.4)
391.      1009 FORMAT(8E15.8)
392.      CALL EXIT
393.      END
```


ORIGINAL PAGE IS
OF POOR QUALITY

RIBBON

145
146
147
148
149
150
151
152
153
154
155
156
157
158
159
160
161
162
163
164
165
166
167
168
169
170
171
172
173
174
175
176
177
178
179
180
181
182
183
184
185
186
187
188
189
190
191
192
193
194
195
196
197
198
199
200
201
202
203
204
205
206
207
208
209
210
211
212
213
214
215
216
217
218
219
220

```

END IF
I1= I
I= I+1
DO 65 J= 0,NS
65 ISR(I,J)= ISR(I1,J)
IF (H(IB)-XS(L).GT. 1.D-4) THEN
IXSL= XS(L)
ISR(I,IXSL)= -ISR(I,IXSL)
ELSE
X(I)= H(IB)
IB= IB+1
ISR(I,0)= IB
GO TO 60
END IF
70 CONTINUE
DO 80 L= IB,NS
IF (H(L).LT. X(I)) GO TO 81
I1= I
I= I+1
X(I)= H(L)
DO 75 J= 1,NS
75 ISR(I,J)= ISR(I1,J)
80 ISR(I,0)= L+1
81 CONTINUE
LAS= I
IF (X(I).NE. 20) THEN
LAS= I+1
X(LAS)= 20
END IF
LAS= LAS+1
X(LAS)= 30
WRITE(KO,1000)(X(J),J=0,LAS)
WRITE(KO,1001)(XS(J),IXS(J),J=1,K)
WRITE(KO,1002)((ISR(L,J),J=0,NS),L=0,I)
DO 90 I= 1,LAS
K= I
IF((X(I)+LIN).GT. 1.D-8) GO TO 91
90 CONTINUE
91 CONTINUE
KO= K
RA= EMAG**((1.DO/(JN-1))
EL= ELL*(1-RA)/(1-RA**JN)
JNN= JQC+JN+1
KK= 2
DO 110 KKI= 0,K
KKKS= KKI+1
KKK= KKI
IF((H(KKI)+LIN).GE. 0. ) GO TO 111
KK= KKI+1
XR(KK)= SNGL(H(KKI))
YR(1,KK)= SNGL(Y(KKI))
KK= KKI+1
XR(KK)= SNGL(H(KKI))
YR(1,KK)= SNGL(Y(KKKS))
110 CONTINUE
111 KKS= KK
KKS1= KK+1
DO 997 IC= 2,NG
READ(KI,*) IS,HO,KOUT,KOU, EPS,A,B,V,POMIN,POMAX,CMIN,CMAX
WRITE(KO,82) IS,HO,KOUT,KOU, EPS,A,B,V,POMIN,POMAX,CMIN,CMAX
KOUT= 6 FOR PRINTED STRESS DATA
KOU > 0 FOR PUNCHED STRESS DATA
82 FORMAT('O IS= ,I3, HO= ,E12.5,
1 KOUT= ,I3, KOU= ,I3, EPS= ,E12.5, A= ,E12.5,
2 E12.5, V= ,E12.5, POMIN= ,D25.18, POMAX= ,D25.
3 E12.5, CMIN= ,D25.18, CMAX= ,D25.18)
READ(KI,*) (TS(I),I=1,NS1)
WRITE(KO,6) (TS(I),I=1,NS1)
6 FORMAT('OTS= ,/(D14.4))
DO 83 I= 0,NS1
TS(I)= TS(I)*TMR
TS4(I)= TS(I)**4
83 CONTINUE
IS1= MOD(1-IS,JQC)

```